Arch. Mech., 34, 5-6, pp. 563–579, Warszawa 1982

Experimental analysis of sloshing flow in circular cylindrical tank using the laser Doppler velocimeter

A. CENEDESE (ROME)

BY MEANS of a laser Doppler velocimeter the flow field of a liquid contained in a circular cylinder tank excited by a sinusoidal force of a given frequency and amplitude was analysed. An out-of-phase between the velocity in different points of the field is shown as an effect of the fluid viscosity; as a consequence of this, the measured velocity in some points is less than that taken from the bottom of the tank. For high values of the excitation force the analysis of the velocity spectrum shows nonlinear effects such as: frequencies which are multiple of the excitation frequency, frequency line spread out, appearance of turbulent phenomena.

Za pomocą dopplerowskiego prędkościomierza laserowego zbadano pole przepływu w cieczy zawartej wewnątrz kołowego zbiornika cylindrycznego, pobudzonej obciążeniem sinusoidalnym o danej częstości i amplitudzie. Pokazano, że niezgodność w fazie między prędkościami w różnych punktach obszaru wynika z lepkości cieczy. W rezultacie prędkość mierzona w różnych punktach jest mniejsza od prędkości obserwowanej na dnie zbiornika. Przy dużych wartościach siły wymuszającej analiza widma prędkości wykazuje szereg zjawisk nieliniowych, takich jak częstotliwości będące wielokrotnościami częstotliwości wymuszającej lub pojawianie się efektów turbulencyjnych.

При помощи доплеровского лазерного скоростемера исследовано поле течения в жидкости, содержавшейся внутри кругового цилиндрического резервуара, возбужденного синусоидальной нагрузкой с данной частотой и амплитудой. Показано, что несовпадение в фазе между скоростями в разных точках области следует из вязкости жидкости. В результате скорость измеряемая в разных точках меньше чем скорость наблюдаемая на дне резервуара. При больших значениях вынуждающей силы анализ спектра скорости указывает на ряд нелинейных явлений, таких как частоты, будучие многократностями вынуждающей частоты или появление турбулентных эффектов.

Nomenclature

a	radius of the circular cylindrical tank,
F	maximum value of the acting force,
f	frequency of the acting force,
g	gravity acceleration,
h	height of the liquid at rest,
h_n	distance from the gravity center of the liquid mass of the n-th spring-mass system in the equivalent mechanical model,
J_1	Bessel function,
k_n	elastic constant of the n-th spring in the equivalent mechanical model,
m_L	total liquid mass,
m_n	n-th mass in the equivalent mechanical model,
r, θ, z	cylindrical coordinates,
T	integration time interval,
t	time,

u horizontal component of velocity,
u_b horizontal component of velocity of the liquid at the bottom of the tank outside of the Stokes layer,
u_t horizontal component of velocity of the tank,
v vertical component of velocity,
X_0 maximum lateral displacement,
α out-of-phase,
β_n damping coefficient,
ε roots of equation $J_1'(\varepsilon) = 0$,
ϱ density,
Φ velocity potential,
Ω circular frequency of the acting force,
ω circular frequency of the natural mode.

1. Introduction

A CONSIDERABLE percentage of the weight of airplanes and space vehicles is made up of liquid fuel contained in the tanks. The force acting by the liquid on the structure is therefore particularly significant if the frequency with which the tank is excited is close to the natural frequency of the liquid-tank system. Knowledge of this phenomenon is necessary for making stability and structural investigations, therefore numerous analytical and experimental studies were carried out on this subject [1, 2, 3, 4].

The particular characteristics of the fluid motion, where the velocity oscillates around the zero value, have made it difficult to analyse the fluid dynamic field experimentally. Experiments on the sloshing flow have been carried out essentially by means of [5, 6]:

capacitance wires;

floating accelerometers held by a wire able to follow the free surface movements;

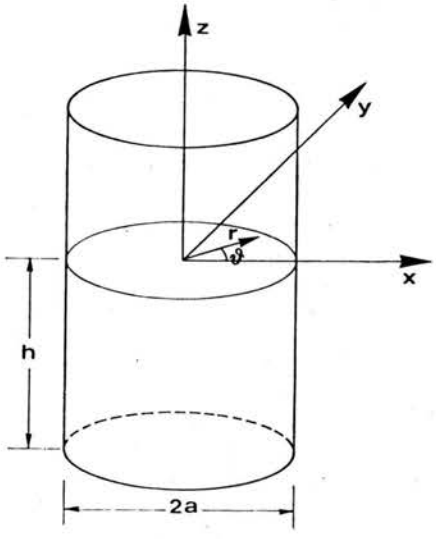

FIG. 1. Tank geometry and coordinate system.

pressure transducer, fixed on the sides of tank, or inside the liquid;
load cells fixed on the tank bottom.

Some of the difficulties met in measuring the velocity field within the oscillating flow are overcome by using the laser-Doppler velocimeter (L.D.V.) [7, 8].

A circular cylindrical tank laterally excited by an oscillating force of a given frequency and amplitude is analysed in the present study by means of the L.D.V. technique. Geometrical parameters and the coordinate system are shown in Fig. 1.

2. Linear theory and equivalent mechanical model

With the assumption of: rigid tank; homogeneous, incompressible and nonviscous fluid; small displacements; the velocity potential $\Phi(r, \theta, z, t)$ satisfies the Laplace equation [9, 10, 11]:

$$\nabla^2 \Phi = 0 \tag{2.1}$$

with the boundary conditions:

(2.2) at the walls $r = a$ $$\frac{\partial \Phi}{\partial r} = i\Omega X_0 e^{i\Omega t}\cos\theta,$$

(2.3) at the bottom $z = -h$ $$\frac{\partial \Phi}{\partial z} = 0,$$

(2.4) at the free surface $$\frac{\partial^2 \Phi}{\partial t^2} + g\frac{\partial \Phi}{\partial z} = 0,$$

Ω is the angular frequency of the force acting on the tank and X_0 is the maximum displacement. It is possible to find closed form solutions by the separation of variables and eigenvalues and eigenfunctions determination:

$$\Phi = i\Omega a X_0 e^{i\Omega t}\cos\theta \left\{ \frac{r}{a} + \sum_{n=1}^{\infty} \frac{2\Omega^2 \cosh\left[\frac{\varepsilon_n}{a}(z+h)\right] J_1\left(\varepsilon_n \frac{r}{a}\right)}{(\varepsilon_n^2 - 1)(\omega_n^2 - \Omega^2)\cosh\left(\varepsilon_n \frac{h}{a}\right) J_1(\varepsilon_n)} \right\}, \tag{2.5}$$

where ω_n is the natural angular frequency:

$$\omega_n^2 = \frac{g}{a}\varepsilon_n \tanh\left(\varepsilon_n \frac{h}{a}\right) \tag{2.6}$$

and where ε_n are the roots of the equation:

$$J_1'(\varepsilon_n) = 0. \tag{2.7}$$

It is possible to consider a mechanical model equivalent to the sloshing flow as an assemblage of springs and masses positioned in such a way as to obtain equal values of the oscillation frequency, the mass and inertial characteristics and the force and moment resultants between the two systems (Fig. 2) [11, 12]. Since the liquid near the top is only slightly disturbed by free surface oscillations, the model consists of a fixed mass which represents essentially a part of the liquid unaffected by sloshing, and a series of movable

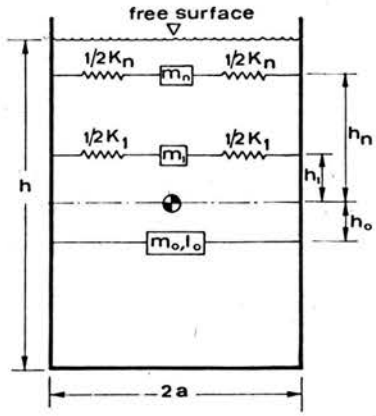

FIG. 2. Equivalent mechanical model.

masses joined to the tank by springs, one for each of the infinite number of sloshing modes of the liquid. The sum of both the fixed and movable masses is equal to the total liquid mass m_L and the ratio between the movable masses and the total mass increases as the liquid content in the tank is lowered. The equation of motion for each oscillating mass and for lateral sloshing is

$$m_n(\ddot{x}_0+\ddot{x}_n)+k_n x_n = 0, \tag{2.8}$$

$$m_0\ddot{x}_0+\sum_{n=1}^{\infty} m_n(\ddot{x}_n+\ddot{x}_0) = -Fe^{i\Omega t}, \tag{2.9}$$

where x_n is the position of n-th mass in a coordinate system fixed with the tank

$$\frac{m_n}{m_L} = \frac{2a\tanh\varepsilon_n \dfrac{h}{a}}{(\varepsilon_n^2-1)\varepsilon_n h}, \tag{2.10}$$

$$\frac{m_0}{m_L} = 1-\sum_{n=1}^{\infty}\frac{m_n}{m_L}, \tag{2.11}$$

$$k_n = m_n\omega_n^2, \tag{2.12}$$

$$\frac{|h_n|}{h} = \left[\frac{1}{2}-\frac{2a}{\varepsilon_n h}\tanh\left(\frac{\varepsilon_n}{2}\frac{h}{a}\right)\right], \tag{2.13}$$

$$\frac{|h_0|}{h} = \frac{m_L}{m_0}\sum_{n=1}^{\infty}\left(\frac{m_n}{m_L}\frac{h_n}{h}\right). \tag{2.14}$$

The mechanical model including linear damping is able to simulate with good approximation the behaviour of the system near the resonant frequencies where an exact solution is practically impossible if the nonlinear effect of the viscosity is taken into account. For the motion of the n-th mass the equation becomes

$$m_n(\ddot{x}_0+\ddot{x}_n)+\beta_n\dot{x}_n+k_n x_n = 0. \tag{2.15}$$

In the expression of the velocity potential Eq. (2.5) the term $(\omega_n^2-\Omega^2)$ is substituted by $\gamma = \sqrt{(\omega_n^2-\Omega^2)^2+\beta_n^2\Omega^2/m_n^2}$ so as to take into account the damping effect even though in linear form.

3. Experimental apparatus

The experimental apparatus (Fig. 3) described in detail in previous studies [13, 14] consists of:

a magnetic vibrator, controlled by a signal generator and a power amplifier, able to exert on an oscillating table a sinusoidal force of given amplitude (0–10 N) and frequency; the apparatus allows a 0.01 Hz sensitivity in the low frequency band;

a laser-Doppler velocimeter with a Bragg cell to shift the frequency in order to measure also velocities close to zero and/or negative.

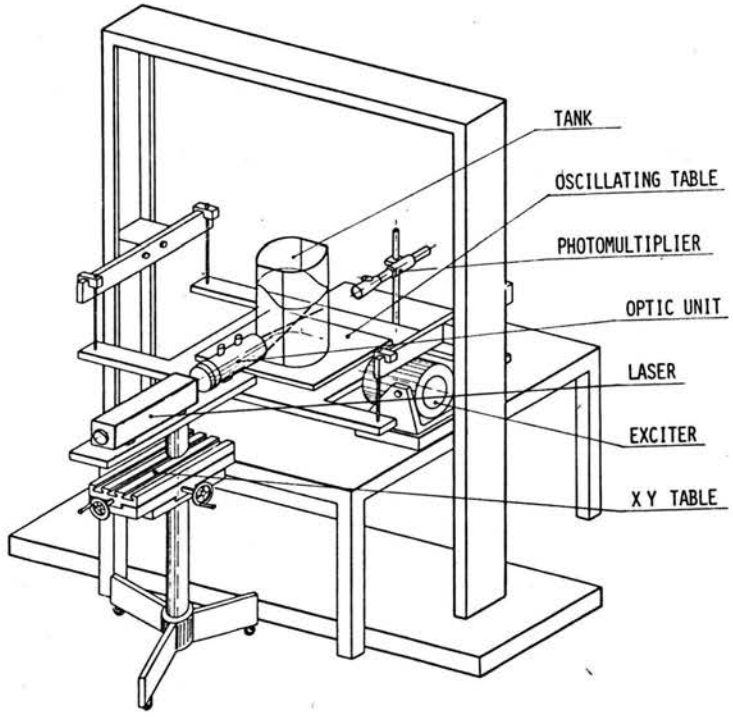

FIG. 3. Experimental set-up.

The tank is made of Plexiglas. When the laser beams meet moving curved surfaces, their intersection point in the liquid moves with reference to a coordinate system fixed within the velocimeter. In order to avoid this inconvenience, two plane windows are made in such a way that the two beams always meet a plane surface throughout the oscillating movement (Fig. 4).

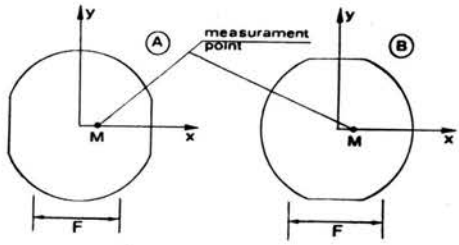

FIG. 4. Tank geometry with plane windows: A) configuration with windows perpendicular to the acting force; B) configuration with windows parallel to the acting force.

In order to verify that the behaviour of the tank with the plane windows is similar in the two tank geometries A and B of Fig. 3 and equal to that in which the cylinder has a fully circular section, the RMS values of vertical velocity

$$\bar{\bar{v}}^2 = \frac{1}{T}\int_0^T v^2(t)dt \tag{3.1}$$

are measured in M (2 cm, 0.2 cm) as the forcing frequency varies. T is a time interval one order larger than the oscillating period. As shown in Fig. 5 and Table 1, the natural frequencies are in good agreement in the two cases and are close to the frequency obtained from the linear theory.

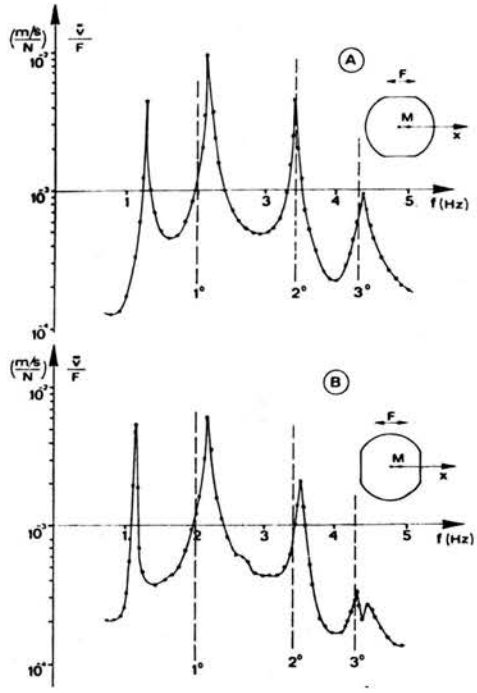

FIG. 5. RMS values of the vertical component of velocity versus acting force frequency at the point M for the two configurations A) and B).

Table 1

	1°	2°	3°
Linear Theory	1.99	3.40	4.31
Case A	2.15	3.40	4.35
Case B	2.20	3.50	4.32

The first natural frequency experimentally determined is greater than that calculated by the linear theory since the viscous effects near the walls cause a reduction of the fluid mass freedom of movement; as if the tank were of a smaller size. The peak which appears at 1.15 Hz is due to the particular geometry of the oscillating table which is suspended by four vertical steel cables to a rigid structure. Therefore the frequency of 1.15 Hz is that characteristic of the system considered as a simple pendulum. The introduction of the plane windows has little effect on the genesis of the natural oscillation modes, while it has a considerable effect as far as the swirling motion is considered, in fact in the present arrangement such motion does not take place even for high values of the excitation forces.

4. Analysis of the results

1.

Figure 6 shows the behaviours of the RMS values of vertical velocity $\bar{\bar{v}}$, 2 cm below the free surface at rest along the X-axis for the first three natural modes. The linear theory gives

$$v = i\Omega X_0 e^{i\Omega t}\cos\theta \cdot \sum_{n=1}^{\infty} \frac{2\varepsilon_n \Omega^2 J_1\left(\varepsilon_n \frac{r}{a}\right) \sinh\left[\frac{\varepsilon_n}{a}(z+h)\right]}{(\varepsilon_n^2-1)J_1(\varepsilon_n)\cosh\left(\varepsilon_n \frac{h}{a}\right)(\omega_n^2-\Omega^2)}. \tag{4.1}$$

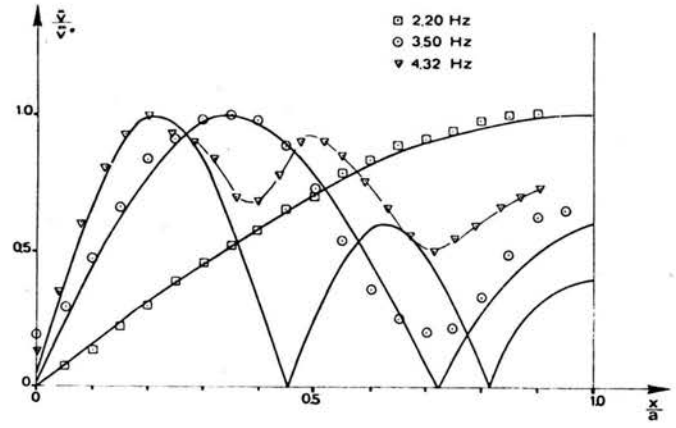

FIG. 6. Horizontal profile of the RMS values of the vertical component of velocity for the first three natural modes.

In the case of real fluids the viscosity causes a damping effect so that with relation to the m-th mode, where $\Omega = \omega_m$, the velocity values remain finite. The term $(\omega_m^2 - \Omega^2)$ of Eq. (4.1) may be substituted by another term γ which takes into account the damping effect:

$$(4.2) \quad v = i\Omega X_0 e^{i\Omega t}\cos\theta \cdot \left\{ \left[\frac{2\varepsilon_n \Omega^2 J_1\left(\varepsilon_m \frac{r}{a}\right) \sinh\left[\frac{\varepsilon_m}{a}(z+h)\right]}{(\varepsilon_m^2 - 1) J_1(\varepsilon_m) \cosh\left(\varepsilon_m \frac{h}{a}\right) \gamma} \right] + \sum_{\substack{n=1 \\ n \neq m}}^{\infty} \left[\frac{2\varepsilon_n \Omega^2 J_1\left(\varepsilon_n \frac{r}{a}\right) \sinh\left[\frac{\varepsilon_n}{a}(z+h)\right]}{(\varepsilon_n^2 - 1) J_1(\varepsilon_n) \cosh\left(\varepsilon_n \frac{h}{a}\right) (\omega_n^2 - \Omega^2)} \right] \right\},$$

γ is different from zero, but small with respect to the terms $(\omega_n^2 - \Omega^2)$ with $m \neq n$; the m-th term of Eq. (4.2) is one order of magnitude greater than the other terms, so that

$$(4.3) \quad \frac{\bar{\bar{v}}}{\bar{\bar{v}}^*} = \frac{\left| J_1\left(\varepsilon_m \frac{r}{a}\right) \right|}{J_1\left(\varepsilon_m \frac{r^*}{a}\right)},$$

where r^* is the point in which $\bar{\bar{v}}$ takes the maximum value corresponding to the first zero point of $J_1'\left(\varepsilon_m \frac{r}{a}\right)$.

For the first natural mode the theoretical value of vertical velocity is maximum where $r = a$. It is not possible to take measurements near the wall because of the tank oscillation. However, the two measurements taken nearest to the wall (the last at about 1 cm) give almost identical RMS values. Thus the maximum value of the velocity is found for $r < a$ owing to a boundary layer effect.

Likewise for the second natural mode the viscosity effect near the wall causes the nodes and the maxima to move towards the center of the tank. The third mode is less easily isolated, the RMS behaviour of vertical velocity shows a coupling between this mode and the first two modes.

2.

Because of viscosity the oscillation amplitude near the natural frequency is finite and furthermore viscosity causes an out-of-phase between the tank velocity u_t and the fluid velocities within the tank.

For $\Omega = \omega_m$ one has

$$(4.4) \quad u = \sqrt{2} B \cos\Omega t + \sqrt{2} A \cosh\zeta \cos[\Omega t - \alpha(x, y)],$$

where

$$(4.5) \quad \zeta = \frac{\varepsilon_m}{a}(z+h),$$

$$B = \frac{\Omega X_0 \cos\theta}{2}, \tag{4.6}$$

$$A = \frac{\sqrt{2} J_1\left(\varepsilon_m \frac{r}{a}\right) \Omega^3 X_0 \cos\theta}{(\varepsilon_m^2 - 1) J_1(\varepsilon_m) \cosh\left(\varepsilon_m \frac{h}{a}\right) \gamma} \tag{4.7}$$

The velocity u is given by the sum of two terms: the first one due to the motion of the rigid body; the second one, due to the free surface oscillation, is out of phase with respect to the first by a term $\alpha(x, y)$. The RMS value of u is given by

$$\bar{\bar{u}}^2 = B^2 + A^2 \cosh^2\zeta + 2AB \cosh\zeta \cos\alpha. \tag{4.8}$$

The effective value of the horizontal component of velocity close to the bottom of the tank goes from the value $A+B$ at an elevation given by $\sqrt{\nu/\Omega}$ (where a Stokes motion can be assumed) to the value B at the bottom of the tank. If no slip conditions are considered, $\alpha(x, y) = 0$ on the walls.

The term A is always smaller then B. Moving upwards α becomes different from zero and the $\bar{\bar{u}}$ value may be less than that at the tank bottom as long as the value of $A\cosh\zeta$ remains smaller than or of the same order of magnitude as B (Fig. 7).

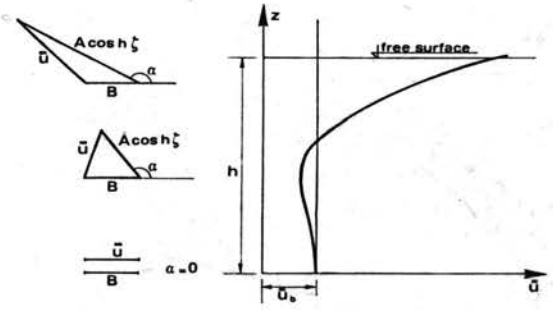

FIG. 7. Behaviour of the vertical profile of the RMS values of the horizontal component of velocity, taking into account the out-of-phase between the liquid and the tank velocity.

The minimum value of $\bar{\bar{u}}$ is reached at the height ζ^* which depends on α and on the other characteristic parameters of the phenomenon by the relationship

$$B\cos\alpha = -A\cosh\zeta^*. \tag{4.9}$$

For the first three natural modes the distribution of u along a vertical 2 cm from the tank axis has been measured. From the linear theory one has

$$\eta(\zeta) = \frac{\bar{\bar{u}} - \bar{\bar{u}}_b}{\bar{\bar{u}}_t - \bar{\bar{u}}_b} = \cosh\zeta - 1, \tag{4.10}$$

where u_b is the liquid horizontal velocity at the bottom of the tank outside of the Stokes layer.

The experimental values obtained are shown in the diagrams of Figs. 8, 9 and 10 in terms of

$$\eta^*(\zeta) = (\bar{\bar{u}} - \bar{\bar{u}}_b) H, \tag{4.11}$$

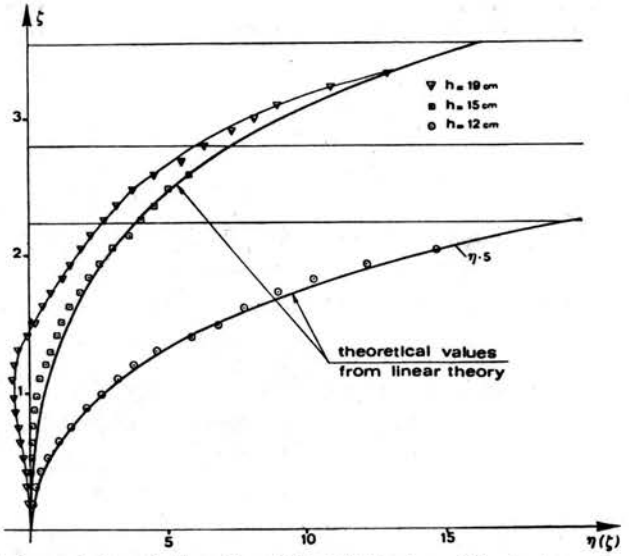

FIG. 8. Observed and theoretical vertical profiles of the RMS values of the horizontal component of velocity for the first natural mode (2.20 Hz) for three different heights of the liquid.

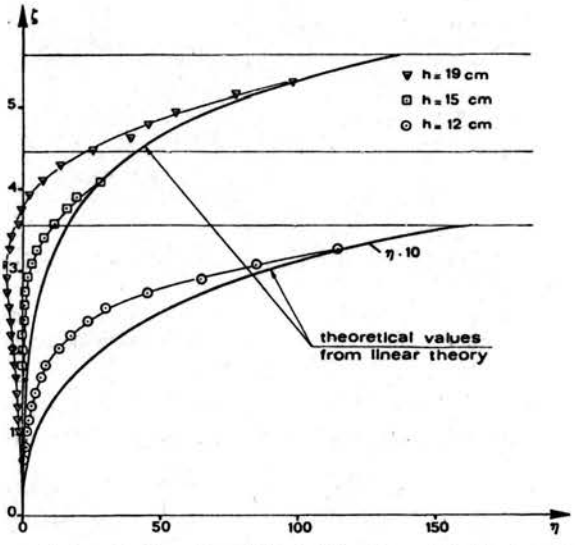

FIG. 9. Observed and theoretical vertical profiles of the RMS values of the horizontal component of velocity for the second natural mode (3.50 Hz) for three different heights of the liquid.

where H is a constant calculated in such a way as to obtain an equality between η and η^* in the nearest free surface point where measuring is possible, that is about 1 cm below free surface at rest.

For three different levels of the liquid contained in the tank and for the same values of the exciting force the behaviour of $\overline{\overline{u}}$ for the first vibration mode (2.20 Hz) is shown in Fig. 8. Only for the highest value of h (19 cm) the velocity out of phase is evident; in

the other two cases observed ($h = 15$ cm and $h = 12$ cm) a good agreement between theoretical and experimental values is obtained. For the second and third vibrations modes the out-of-phase effect is more noticeable (Figs. 9 and 10).

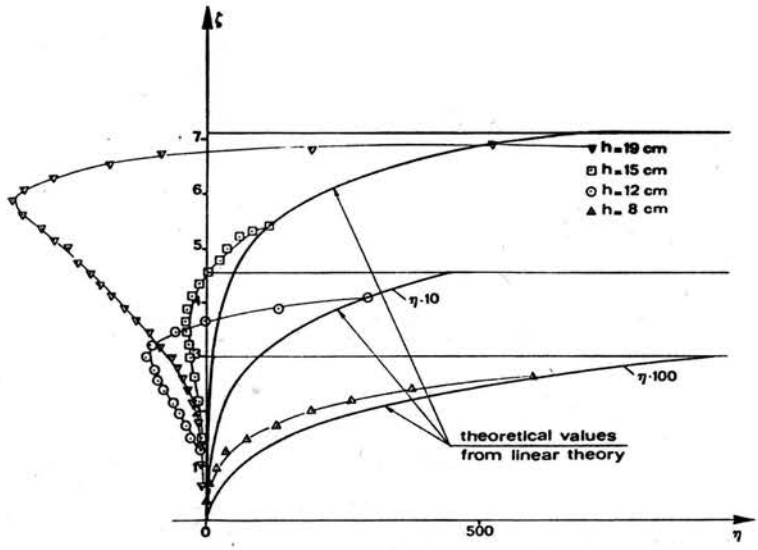

FIG. 10. Observed and theoretical vertical profiles of the RMS values of the horizontal component of velocity for the third natural mode (4.32)Hz for four different heights of the liquid.

3.

The RMS values of v in M as a function of the maximum value of the acting force F are shown in Fig. 11 for the first three vibration modes. There exists a range of values of F where the ratio $\bar{\bar{v}}/F$ is constant, this range is greater for the higher level modes.

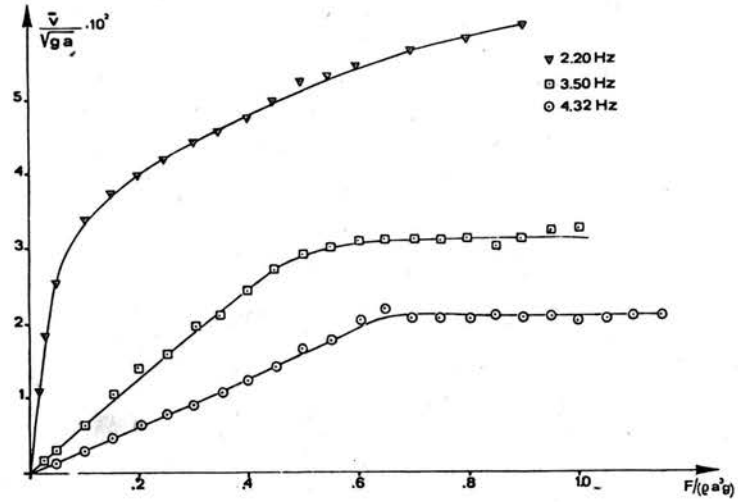

FIG. 11. RMS values of the vertical component of velocity as a function of the acting force at M for the first three natural modes.

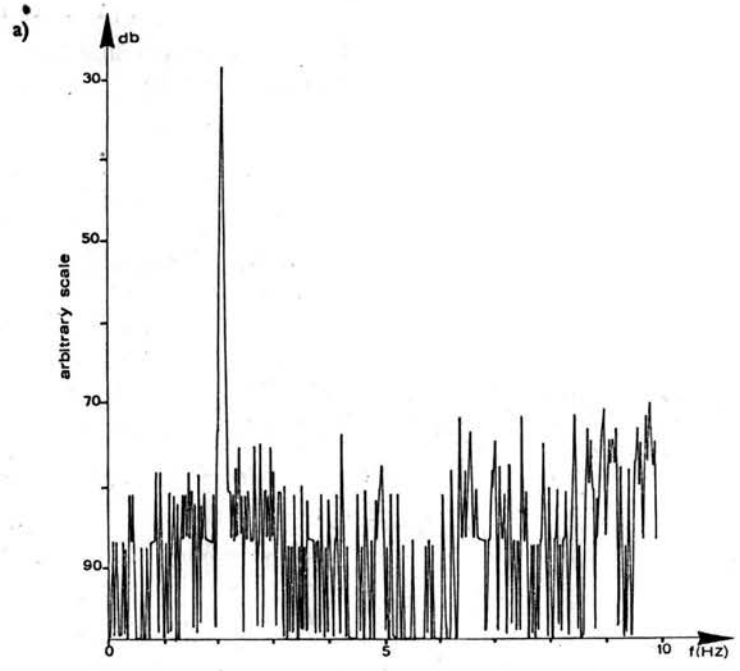

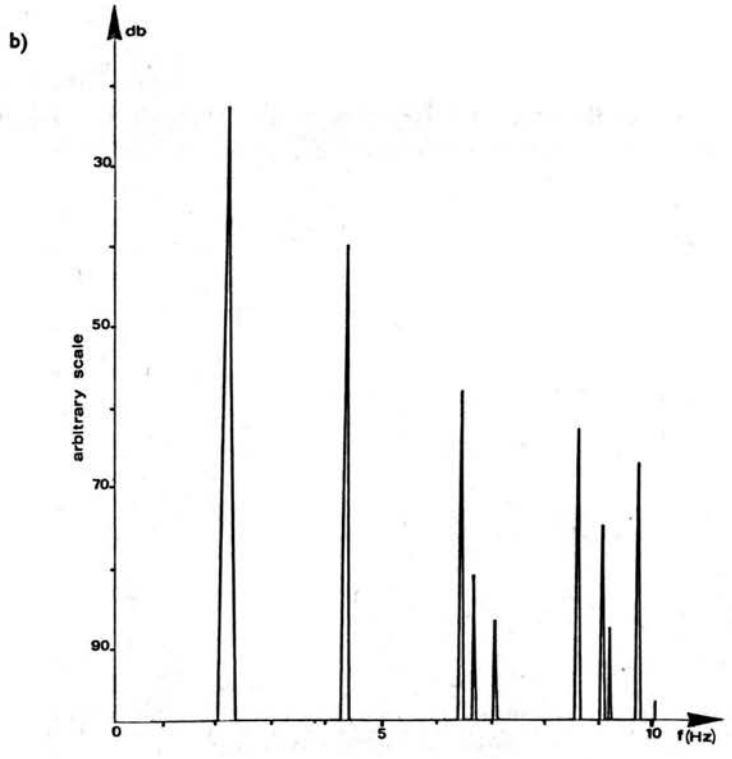

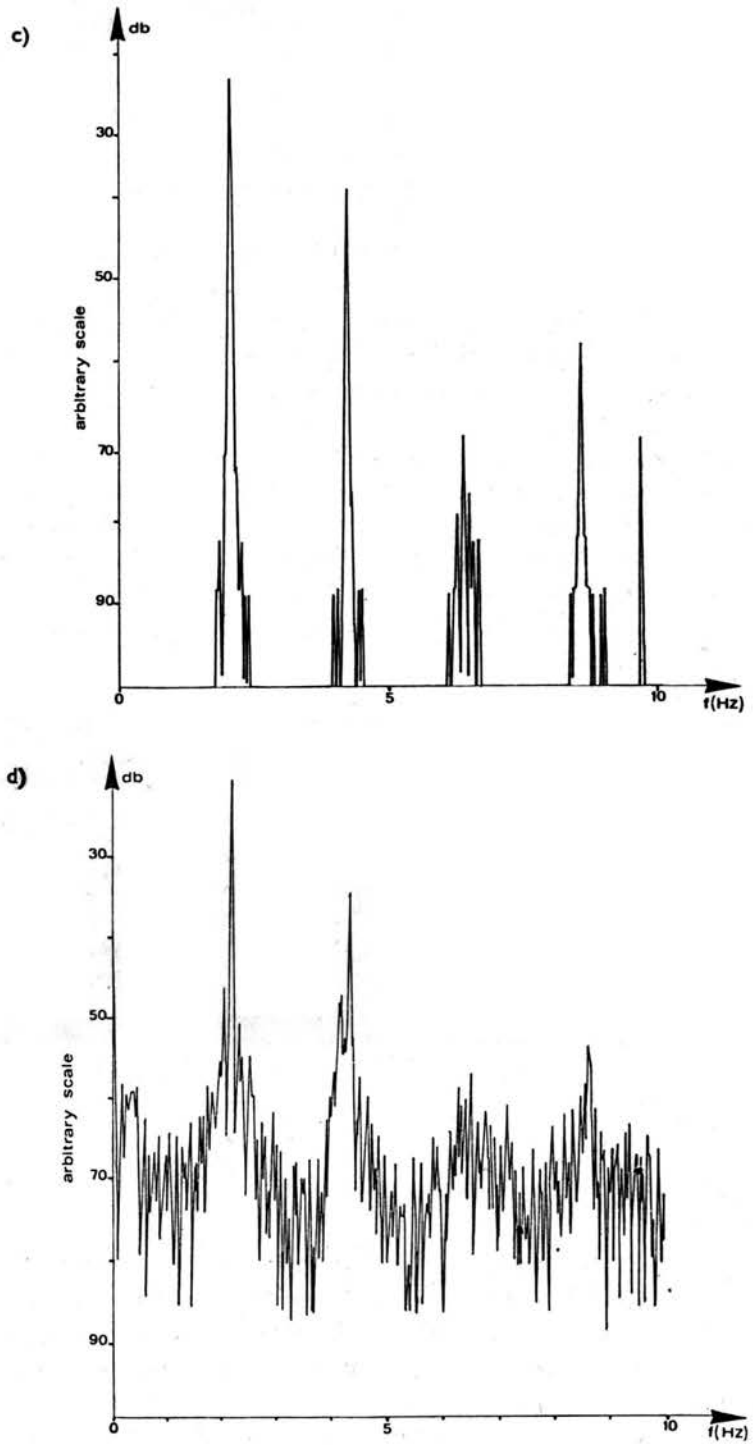

FIG. 12.a) Power spectrum of the vertical component of velocity at the point M due to an acting force of 1.0 N for the first natural mode. b) Power spectrum of the vertical component of velocity at the point M due to an acting force of 2.0 N for the first natural mode. c) Power spectrum of the vertical component of velocity at the point M due to an acting force of 4.0 N for the first natural mode. d) Power spectrum of the vertical component of velocity at the point M due to an acting force of 6.0 N for the first natural mode.

The spectrum analysis of the vertical component of velocity at point M has been obtained by a real time spectrum analyser using the F.F.T. As the exciting force increases, the spectrum analysis shows a different mode of energy distribution in the frequency domain. Four typical situations are shown:

a) in the range where F is small and the ratio $\bar{\bar{v}}/F$ is constant, the energy is concentrated around the exciting frequency;

b) as F increases, a coupling between different harmonics appears, whose frequencies are multiple of the fundamental one: this is the typical behaviour of a nonlinear system;

c) for higher values of F the peaks corresponding to the harmonics multiple of the fundamental one spread out;

d) for even higher values of the exciting force a discrete periodic spectrum appears to be superimposed to a continuous spectrum which is a typical turbulence phenomenon.

The four behaviour patterns are shown in Fig. 12 for the first vibration mode. The photos of Fig. 13 show the velocity distribution where $\bar{\bar{v}}/F$ is constant and where turbulent phenomena appear. A similar behaviour is shown in the spectra of Fig. 14 for the second vibration mode; in this last case, for the examined force range, turbulent phenomena do not appear.

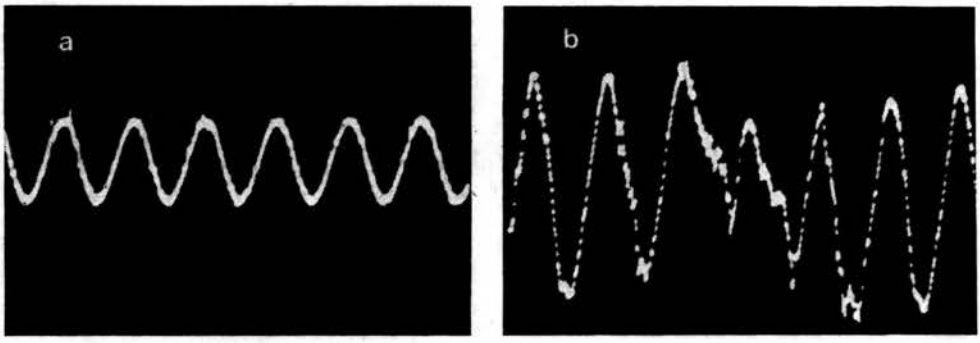

FIG. 13. a) Time distribution of the vertical component of velocity where no turbulent phenomena appear. b) Time distribution of the vertical component of velocity where turbulent phenomena appear.

5. Conclusions

With the use of the Laser Doppler Velocimeter it is possible to analyse the fluid dynamics field in the liquid contained in an oscillating tank without disturbing the flow and with an excellent spatial resolution. The results obtained are in good agreement with those foreseen by the linear theory with regard to the natural frequencies and the qualitative velocity behaviour.

Considering the horizontal velocity RMS along a vertical, it is possible to show an out-of-phase of velocity at different points. This phenomenon is particularly evident for high water levels in the tank and for higher orders of vibration modes. Thus, in some points of the tank, RMS values of velocity are lower than those measured near the bottom.

The velocity spectra taken near the tank center show for the lowest values of the

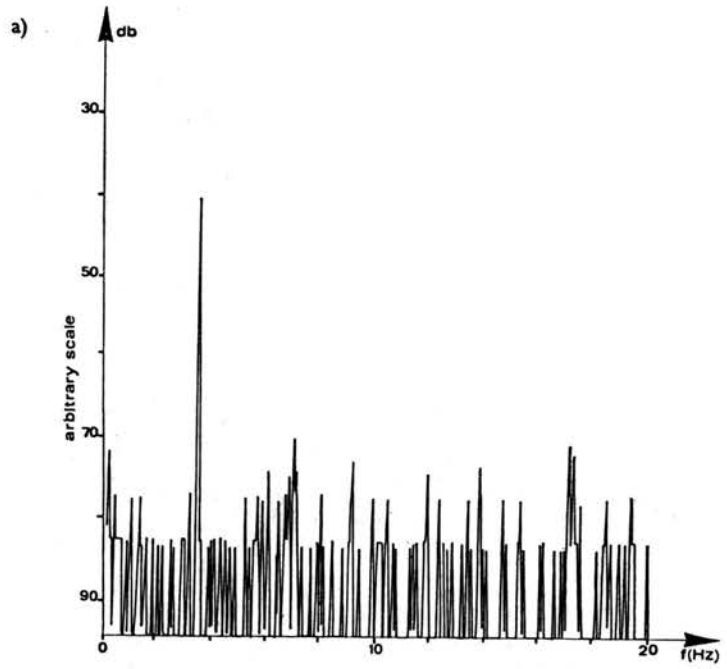

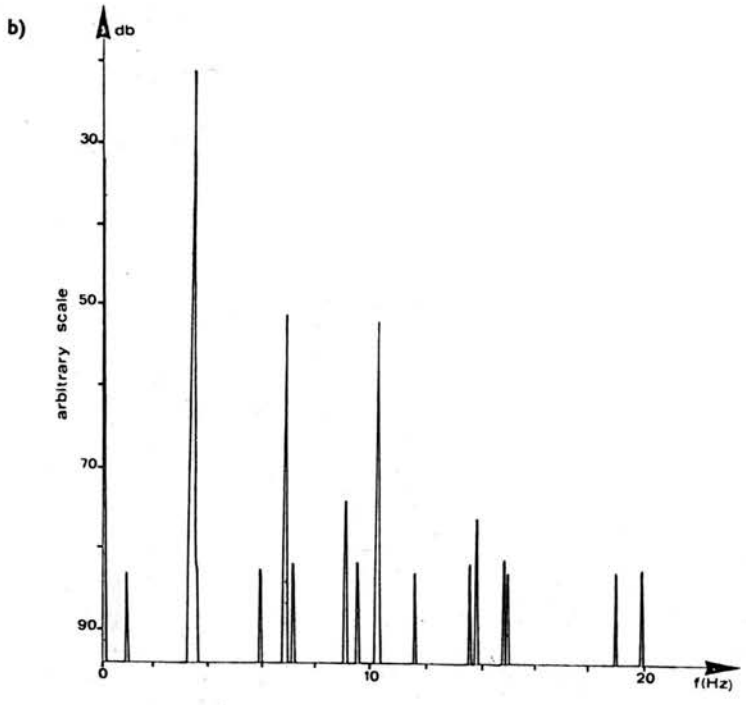

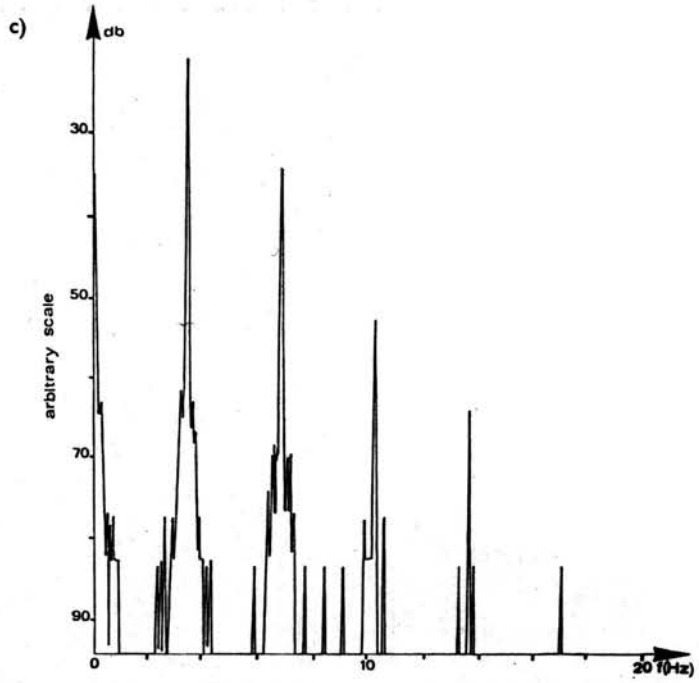

FIG. 14. a) Power spectrum of the vertical component of velocity at the point M due to an acting force of 1.0 N for the second natural mode. b) Power spectrum of the vertical component of velocity at the point M due to an acting force of 3.0 N for the second natural mode. c) Power spectrum of the vertical component of velocity at the point M due to an acting force of 6.0 N for the second natural mode.

exciting force only one peak at the forcing frequency. As the exciting forces gradually increase, nonlinear effects become evident and frequences which are multiple of the forcing one appear. Then a peak spread-out around $m\omega_n$ values takes place. For the highest values of the exciting force one has an overlapping between a periodic discrete spectrum and a continuous spectrum which shows the appearance of turbulent phenomena.

Acknowledgment

The author is grateful to Prof. P. SANTINI, director of the "Istituto di Tecnologia Aerospaziale", for having made available a part of the experimental apparatus. The author is also grateful to Prof. D. CUNSOLO, Prof. M. MARCHETTI, Prof. M. OTTAVIANI and G. SICLARI, for useful discussions.

References

1. H. N. ABRAMSON, *The dynamic behaviour of liquid in moving containers*, NASA SP-106, 1966.
2. P. SANTINI, R. BARBONI, *Motion of orbiting spacecrafts with a sloshing fluid*, Acta Astronautica, **5**, 1978.

3. F. PFEIFFER, *Problems of containing rotating fluid with respect to aerospace application*, ESA SP-129, 1977.
4. R. VALDIN, R. OHAYON, *Influence du ballottement dans les reservoir des bouts d'ailes sur les modes propres de vibrartion d'un avion*, ICAS Paper, 1974.
5. I. E. SUMMER, A. J. STOFAN, *An experimental investigation of viscous damping of liquid sloshing in spherical tanks*, NASA TN D-1991. 1963.
6. J. F. DALZELL, *Simulation and experimental technique of liquid sloshing*, NASA SP-106, 1966.
7. F. DURST, A. MELLING, J. H. WHITELAW, *Principles and practice of laser anemometry*, Academic Press 1975.
8. T. S. DURRANI, C. A. GREATED, *Laser systems in flow measurement*, Plenum Press 1977..
9. H. LAMB, *Hydrodynamics*, Dover Publ., 1945.
10. S. SILVERMAN, H. N. ABRAMSON, *Lateral sloshing in moving containers*. NASA SP-106, 1966.
11. J. R. ROBERTS, E. R. BASURTO, PEI-YING CHEN, *Slosh design handbook*, NASA CR-406, 1966.
12. F. T. DODGE, *Analytical representation of lateral sloshing by equivalent models*, NASA SP-106, 1966.
13. A. CENEDESE, M. MARCHETTI, G. SICLARI, *Analisi sperimentale del moto di un liquido in un serbatoio parallelepipedo oscillante*, XVII Convegno di Idraulica e Costruzioni Idrauliche, Palermo 1980.
14. A. CENEDESE, *Oscillating flow in prismatic tanks: experimental analysis*, XIX IAHR Congress, New Delhi 1981.

AERODYNAMIC INSTITUTE
ROME UNIVERSITY, ROME, ITALY.

Received November 16, 1981.